Theoret. Comput. Fluid Dynamics (1998) 10: 201–212

Theoretical and Computational Fluid Dynamics

Natural Disasters: Explosive Volcanic Eruptions and Gigantic Landslides[1]

Herbert E. Huppert and W. Brian Dade

Institute of Theoretical Geophysics,
Department of Applied Mathematics and Theoretical Physics,
Silver Street, Cambridge CB3 9EW, England
heh1@esc.cam.ac.uk and bdade@esc.cam.ac.uk

Communicated by M.Y. Hussaini

Received 4 January 1997 and accepted 12 May 1997

Abstract. The 1990s have been designated the International Decade of Natural Disaster Reduction; and this paper discusses two natural disasters. In the first we show how to model massive, ground-hugging ash flows, known as pyroclastic flows by geologists, in terms of particle-driven, turbulent gravity currents. A framework for solving forward problems is set up so that, for different geometries, all the flow and deposit properties can be predicted given the initial conditions of the flow following a volcanic eruption. This is then used to discuss inverse problems, for which only the details of the deposit are provided and the initial conditions of the flow are to be calculated. This method of approach is applied to analysing the eruption of Taupo, New Zealand, about 1800 years ago. We demonstrate that the ash-laden flow travelled over the ground in a current of order 1 km high travelling at a typical speed of 200 m s^{-1}.

The second study concerns the runout of massive landslides. A model employing the concepts of the flow of granular materials is presented in which the interior of the rockfall propagates uniformly above a thin shear layer of rocks through which all the rocks eventually fall, to leave the flow and add to its deposit. Quantitative predictions from this theoretical model are shown to agree well with observations from about 50 rockslides on Earth, the Moon and Mars. Our model suggests that simulation of such granular flows would be extremely difficult, if not impossible, to achieve in the laboratory.

1. Introduction

James Lighthill has used his enormous intellectual talents to create a number of completely new fields, including the areas of noise produced aerodynamically, biofluiddynamics, and non-linear acoustics. In addition, he has been extremely influential in a variety of roles such as Director of the Royal Aircraft Establishment at Farnborough, Provost of University College, London and a Director of the Post Office. Recently, as Chairman of the Special Committee on the International Decade for Natural Disaster Reduction, James has caused its members to think quantitatively and clearly about natural disasters, and at the same time has contributed immensely to the scientific debate (Lighthill *et al.*, 1993; Lighthill, 1996). In the spirit of this interest, we present in honour of James a summary of two studies we have recently undertaken on hazardous flows.

[1] The research of the authors is supported by grants from the Leverhulme Foundation and NERC.

The first concerns the product of large volcanic eruptions, which can lead to what geologists call a pyroclastic flow: a hot, ground-hugging ash flow which is generated by the collapse of a volcanic eruption column. Volcanic eruptions represent one of the most destructive natural disasters in terms of mortality in a variety of different ways. For example, 22,000 people were swept away as a result of mud slides following the eruption of Nevado del Ruiz, Colombia in 1985; 29,000 people were asphyxiated following the eruption of Mount Pelée in the West Indies in 1902; and 35,000 people died, mainly through drowning, due to the famous eruption of Krakatau, Java in 1883. In this century property damage of more than $ 10,000 million has occurred as a result of volcanic eruptions. (More details can be found in the stimulating article by Rampino (1992).)

Eruptions originate due to increasing pressure in the liquid chamber beneath the volcanic edifice leading to unsustainable shears in the overlying rock. The rock breaks apart and a vent to the atmosphere from the chamber below is created. A three phase turbulent flow of small solid rock particles, liquid magmatic droplets and released vapour can penetrate into the atmosphere at speeds considerably in excess of the local speed of sound at temperatures around 700 °C (Kiefer, 1977). The upwardly directed momentum of this turbulently moving jet is gradually decreased while at the same time the jet entrains relatively cold, ambient air. The small, heavy and hot ash particles quickly transfer some of their heat to this interstitial air which thereby becomes less dense and thus decreases the effect of the negative buoyancy of the trapped particles. Quantitative models have been constructed (Woods, 1988, 1995) that predict the minimum initial momentum flux necessary for the bulk buoyancy to become positive by this process, which permits the eruption column to rise further into the atmosphere, driven by the thermal exchanges between the hot particles and the entrained air. This leads to what is known as a Plinian eruption column (Pliny, 79). (For interesting additional accounts, see Francis (1993) and some of the references therein.) If the initial momentum flux is not sufficiently high, the column of hot ash particles and entrained air collapses and propagates out along the terrain as a relatively heavy and hot pyroclastic flow. It is this situation we consider here.

We model the hot, pyroclastic flow as an isothermal, turbulently propagating particulate-driven gravity current. We summarize some of the approaches that have been used to investigate this situation in order to predict: the rate of propagation of the current; the distribution of deposited material; and the final runout length. This is what a geophysicist calls a forward problem. The corresponding inverse problem determines the initial conditions of the flow, and especially the initial particulate concentration, given the observed distribution of the deposit. We apply these ideas particularly to the eruption of Taupo, New Zealand, 1800 years ago, which distributed 30 km^3 of solid material across the North Island and was one of the largest eruptions in the last 10,000 years. Specifically, we show that the solids concentration after collapse of the central column was of order 0.3% by volume in a flow whose typical radial velocity was 200 $m\,s^{-1}$.

The second study we review here is a new model for the runout characteristics of large rockfalls, which can constitute spectacular geological hazards. Very large debris avalanches, in which the volume of the transported material is greater than 1 km^3, can run out a horizontal distance greater than ten times the fall height. There are observations of such catastrophic flows on Earth, on the Moon and on Mars. The largest, currently known landslide occurred on Mars had an estimated volume of 18,000 km^3 and ran out about 20 times its initial height of fall (Lucchitta, 1979).

We apply some of the modern concepts of the flow of granular media (Bagnold, 1954; Savage, 1989; Campbell, 1990) to analyse a model in which the interior of the rockfall is considered to propagate uniformly above a thin shear layer of rocks at the base. The volume of the rockfall gradually decreases as rocks fall out of this shear layer, having transferred their momentum to the main flow. Quantitative predictions from our analysis compare well with observations from specific avalanches. One of the most interesting, and probably controversial, aspects of our model is that it indicates that conditions required for long runout would be difficult, if not impossible, to achieve in laboratory settings.

2. Particle-Driven Gravity Currents

2.1. Compositional Currents

Gravity currents occur whenever fluid of one density propagates primarily horizontally into fluid of a different density. A very readable review of gravity currents, along with a series of examples and applications, is given by Simpson (1997). When the density of the current is conserved following the motion, such as when salt

water intrudes into fresh water, the current is called a compositional gravity current. Quantitative studies of inviscid, compositional gravity currents, using the Bernoulli equation, were first carried out by von Kármán (1940) with the arguments corrected somewhat by Benjamin (1968). Their results indicated that if the current intrudes into very deep fluid, the velocity at the front of the current u_N is related to the depth of the current just at the rear of the head h_N by

$$u_N = Fr(g' h_N)^{1/2}, \tag{2.1}$$

where the Froude number Fr is a constant ($\sqrt{2}$ according to perfect fluid theory) and the reduced gravity

$$g' = (\rho_c - \rho_a)g/\rho_a \tag{2.2}$$

in terms of the gravitational acceleration g and the densities ρ_c and ρ_a of the current and ambient, respectively.

An axisymmetric, compositional gravity current, propagating under a balance between inertial and buoyancy forces, can be modelled by the shallow-water equations, which describe the radial velocity and thickness of the current as functions of the radial co-ordinate and time. These equations have a long-time similarity solution (Bonnecaze *et al.*, 1995) for an instantaneous release of a fixed volume, in which the radial extent of the current r_N is given by

$$r_N = C(g'Q)^{1/4} t^{1/2}, \tag{2.3}$$

where t is the time since the release and C is a function of Fr.

This result can be compared with a simple box model that assumes that the initial volume collapses in a series of discs of equal volume, throughout which there are no radial variations. On the assumption that at the front of each disc (2.1) is obeyed (with $\dot{r}_N = u_N$), a result identical to (2.2) is obtained, except that the value of C is slightly altered. Experimental observations agree well with either representation.

2.2. Particulate Currents

If the density difference in the current is due to particulate matter, another variable, the volume concentration of particles, φ, enters the problem. If the density of the interstitial fluid making up the current is the same as that of the ambient ρ_a, while that of the particles is denoted by ρ_p, the density of the current ρ_c is given by

$$\rho_c = \rho_p \varphi + \rho_a(1 - \varphi) \tag{2.4}$$

In this situation another equation must be added that reflects the fact that these particles are advected along with the fluid as well as being sedimented from it through the lower boundary layer. Following earlier studies of sedimentation from turbulent suspensions (Martin and Nokes, 1988), this equation is usually written, for a monodisperse particulate distribution, as

$$\varphi_t + u\varphi_r = -V\varphi/h \tag{2.5}$$

in terms of the radial velocity u, the single particle free-fall speed V and the thickness of the current $h(r, t)$. The resulting shallow-water equations have to be solved numerically (there are no similarity solutions). An extensive numerical investigation was carried out by Bonnecaze *et al.* (1995) and their numerical results agree well with experiments undertaken to test the theoretical model.

2.3. Fixed Volume Box Models

A simple box model for an instantaneous release is described by the following equations (Dade and Huppert, 1995):

$$\pi r^2 h = Q, \tag{2.6}$$

representing conservation of volume;

$$u = \dot{r} = Fr(g'_p \varphi h)^{1/2}, \tag{2.7}$$

where $g'_p = (\rho_p - \rho_a)g/\rho_a$, representing the Froude number condition at the nose; and

$$\dot{\varphi} = -V\varphi/h \tag{2.8}$$

being the r-independent version of (2.5). To the non-linear set (2.6)–(2.8) must be added the initial conditions

$$r = 0, \quad \varphi = \varphi_0 \qquad (t = 0), \tag{2.9a,b}$$

where (2.9a) reflects the assumption that the current is released with small radial extent and φ_0 is the initial (volume) concentration of particles.

Dividing (2.8) by (2.7) and using (2.6) to eliminate h, we obtain

$$d\varphi/dr = -\lambda r^3 \varphi^{1/2}, \tag{2.10}$$

with (2.9) expressed as

$$\varphi = \varphi_0 \qquad (r = 0), \tag{2.11}$$

where

$$\lambda = \pi^{3/2} V/[Fr(g'Q^3)^{1/2}]. \tag{2.12}$$

Equation (2.10) with initial condition (2.11) has solution

$$\varphi^{1/2} = \varphi_0^{1/2} - \tfrac{1}{8}\lambda r^4, \tag{2.13}$$

from which it is immediately seen that the current ceases ($\varphi = 0$) at

$$r_\infty = (8\varphi_0^{1/2}/\lambda)^{1/4}. \tag{2.14}$$

Introducing the non-dimensional variables $\Phi = \varphi/\varphi_0$ and $R = r/r_\infty$, we can rewrite (2.13) as

$$\Phi = (1 - R^4)^2. \tag{2.15}$$

Substituting (2.6) and (2.15) into (2.7) and integrating the result using (2.9a), we find that

$$R = \tanh^{1/2} T \tag{2.16}$$

in terms of the non-dimensional time T given by

$$T = \tfrac{1}{2} Fr(g'_{\rm p}\varphi_0 Q)^{1/2} t/(\pi^{1/2} r_\infty^2). \tag{2.17}$$

These relationships are plotted in Figure 1.

In order to evaluate the deposit distribution, we argue that in time δt the mass $\delta M = -\rho_{\rm p} Q \delta\varphi$ is deposited uniformly over an area of πr^2 to lead to a deposit density

$$\delta\eta = -(\rho_{\rm p} Q/\pi r^2)\delta\varphi. \tag{2.18}$$

Thus the total deposit density (of dimensions ML^{-2}) after the flow has ceased is given by

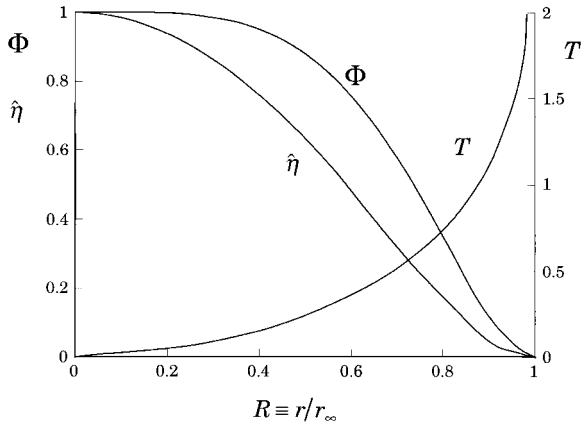

Figure 1. The dimensionless time T, particle concentration Φ and density of deposit $\hat\eta = 3\pi r_\infty^2/(8\rho_{\rm p}\varphi_0 Q)$ as functions of the dimensionless radius R.

$$\eta = -\pi^{-1}\rho_{\rm p} Q \int_{\rm r}^{r_\infty} r^{-2}\varphi_{\rm r}\, dr. \tag{2.19}$$

Differentiating (2.15), substituting the result into (2.19) and carrying out the integration, we find that

$$\eta = 4\rho_{\rm p} Q\varphi_0 (R^6 - 3R^2 + 2)/(3\pi r_\infty^2), \tag{2.20}$$

which is also plotted in Figure 1.

2.4. Fixed Flux Model

We now consider a quasi-steady, axisymmetric particulate gravity current responding to a (point source) input with steady volume flux $\mathcal{F}$. Conservation of volume requires that

$$2\pi r h u = \mathcal{F}. \tag{2.21}$$

In this case of a steady input, there is a balance between particle advection and sedimentation, which indicates that (2.5) can be expressed as

$$u\frac{d\varphi}{dr} = -V\varphi/h. \tag{2.22}$$

Substituting (2.21) into (2.22) and integrating the result subject to the boundary condition (2.11), we obtain

$$\Phi = e^{-\sigma^2}, \tag{2.23}$$

where $\sigma = r/r_*$ is a non-dimensional radial distance defined in terms of the length scale

$$r_* = (\mathcal{F}/\pi V)^{1/2}. \tag{2.24}$$

In contrast to the instantaneous, fixed volume release of the last section, there is not a finite radius at which the mass of particulate matter is completely spent because material is continuously introduced at the source for the duration of the flow.

Substituting (2.21) and (2.23) into the Froude number condition (2.7) at the head of the current, we find that the velocity of the front of the flow satisfies

$$u_N = U_0 \sigma_N^{-1/3} e^{-\sigma_N^2/3}, \tag{2.25}$$

where the velocity scale

$$U_0 = (\tfrac{1}{4}\mathcal{F}VFr^4 g_{\rm p}'^2\varphi_0^2/\pi)^{1/6} \tag{2.26}$$

and σ_N is the value of σ at the front of the current. Since $u_N = \dot{r}_N = r_*\dot{\sigma}_N$, (2.25) can be integrated to yield the time

$$t_N = (r_*/U_0)\int_0^{\sigma_N} x^{1/3} e^{1/3x^3}\, dx \tag{2.27}$$

at which the front of the current is at σ_N.

At any point in the flow the instantaneous downward mass flux of sediment per unit area is given by $\rho_{\rm p}\varphi V$. The local deposit density η is given by the product of this flux and the time of duration of the flow at that point to yield

$$\eta = \rho_{\rm p}\varphi_0 V(t_E - t_N)e^{-\sigma^2} \tag{2.28a}$$

$$= \eta_0(1 - t_N/t_E)e^{-\sigma^2} \tag{2.28b}$$

$$\sim \eta_0 e^{-\sigma^2} \qquad (t_N \ll t_E), \tag{2.28c}$$

in terms of the (observable) density of deposit at the origin η_0 and the total time t_E over which the flux is maintained.

Laboratory confirmation of these relationships is indicated in Figure 2.

2.5. Polydispersed Currents

The above development has concentrated entirely on monodisperse particulate matter, where the free-fall speed is determined by the single constant V. The effects of polydispersion were evaluated both theoreti-

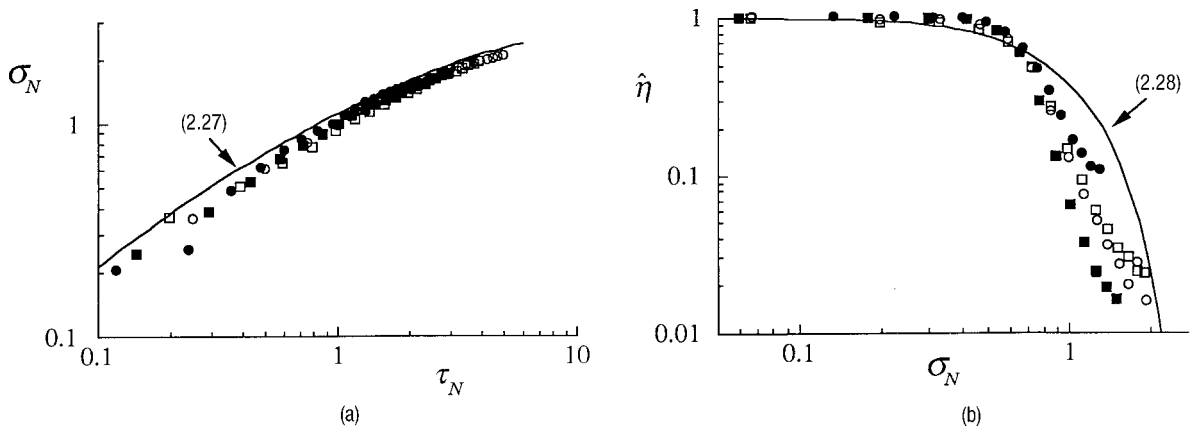

Figure 2. Runout and density of deposit for axisymmetrically spreading particulate gravity currents generated by a constant-flux release. (a) The dimensionless distance to the front of the current $\sigma_N = r_N/r_\star$ as a function of the dimensionless time $\tau_N = U_0 t_N/r_\star$. (b) The dimensionless density of deposit $\hat{\eta} = \eta/[\eta_0(1 - t_N/t_E)]$. Symbols represent experimental data from Bonnecaze *et al.* (1995) and the solid curves represent the theoretically predicted relationships.

cally and experimentally by Bonnecaze *et al.* (1996). Considering the non-linear shallow water equations governing the instantaneous release of a fixed volume containing a number of different particle sizes, they developed a scaling of these equations in such a way that all parameters appeared only in the initial conditions. The long-time solution of these "master" equations was obtained and shown to be independent of all details of the initial conditions except for the total volume. Bonnecaze *et al.* then proposed that the total deposit could be obtained from a direct superposition of the deposit from individual species. The technique was shown to be in good agreement with a series of laboratory experiments using five different particle sizes.

Applying these concepts to the relationship for the density of deposit for a single particle (2.28), on using (2.24), we obtain the relationship

$$\eta(r) = \eta_0 \int_{-\infty}^{\infty} V(\varphi) \exp[-\pi V(\varphi) r^2/\mathcal{F}] p(\varphi)\, d\varphi \Big/ \int_{-\infty}^{\infty} V(\varphi) p(\varphi)\, d\varphi \tag{2.29}$$

in terms of the probability distribution $p(\varphi)$ of particle settling speeds.

2.6. Volcanic Inverse Problems

Sections 2.3 and 2.4 presented the direct, or forward, problems for an instantaneous release or a fixed flux of sedimenting material of one size. For the former, given the initial concentration φ_0 and the parameters that make up λ, the concentration in, position of, and final deposit from the current can be determined. Similarly, these functions can be determined for a fixed flux release given the parameters that make up r_* , U_0, and η_0. A number of complicated models have been constructed (Dobran *et al.*, 1993) which have attempted to include extra effects such as thermal and mechanical non equilibrium between gas and solid phases, particle collisions, and subgrid scale turbulent modelling. The results of these heavily numerical schemes have been applied to forecast the effects of a future eruption of Vesuvius (Dobran *et al.*, 1994).

However, in general, geologists are faced with a different problem. They observe the distribution of the final deposit long after the eruption has ceased and know the particulate distribution within it. From such observations alone they would like to evaluate the strength of the eruption and its duration. They would then like to determine such further quantities as the solids concentration, speed and thickness of the pyroclastic flow as functions of distance.

Such an evaluation, conducted in a quantitative manner, was first carried out by Dade and Huppert (1996) using the results of Sections 2.4 and 2.5.

The deposit from the eruption of Taupo, New Zealand in a.d. 186 has been painstakingly documented after years of work by Wilson (1985). The deposit, called by geologists an ignimbrite, comprises about 30 km^3 of material spread in a roughly axisymmetric fashion around the inferred vent in Lake Taupo over

20,000 km^2 of countryside with little mean slope. The deposit thickness near the vent η_0 is of order 10 m. Using the model of Section 2.4 and 2.5, Dade and Huppert showed that the total volumetric flux $\mathcal{F}$ in the turbulent flow after collapse of the central eruption column was of the order of 40 km^3 s^{-1} and lasted for no more than about 15 minutes. The initial solids concentration in the pyroclastic flow, we infer, was 0.3% by volume in a current that was about 1 km thick and travelled with a typical radial velocity of 200 ms^{-1}. At that speed, by transferring kinetic energy into potential energy, the current could surmount any topographic barriers less than about 2 km in height. All hills within 100 km of Lake Taupo are less than 500 m high and observations confirm that the deposit was draped virtually uniformly over them, further atesting to the enormous energy of the flow. The low solids concentration of 0.3% by volume may seem surprising given the almost opaque nature of contemporary pyroclastic flows. However, particle driven flows of very low concentration in the laboratory also appear opaque, even when viewed quite close up. Further details of the Taupo analysis can be obtained from Dade and Huppert (1996), but it should also be mentioned that their quantitative interpretation is still not accepted by all geologists (Wilson, 1997; Dade and Huppert, 1997).

An even larger eruption occurred at Taupo around 1 million years ago. Approximately 225 km^3 of ash was deposited over 45,000 km^2 (Wilson *et al.*, 1995). Using the concepts described above we calculate that the total initial flux was of order 200 km^3 s^{-1} and that the resulting pyroclastic flow attained its maximum distance from the source of 200 km in less than 20 minutes.

3. Gigantic Landslides

3.1. Simple Models

Many quite small rockfalls can have devastating consequences. Really large landslides released by earthquakes or some other catastrophic event occur less frequently, but have been well documented over the centuries. Enormous rocks can come crashing down the mountainside and travel a distance along the predominantly horizontal valley floor many times the initial fall height. Such events also occur at the sea bed. No generally accepted model has yet been presented to explain the observed characteristics of these very energetic flows.

The simplest model of a rockfall comes from considering a mass M to slide (without tumbling) from a height H down a slope of angle θ, and then to run out along a horizontal plane, as depicted in Figure 3. On the assumption that the (uniform) coefficient of friction $\mu < \tan\theta$, so that sliding can occur, it is easy to show that the horizontal component of velocity U of the mass at the base of the slope is given by

$$U = [2g(1 - \mu/\tan\theta)H]^{1/2}\cos\theta, \tag{3.1}$$

which is dissipated (the mass comes to rest) after a total (slope + floor) *horizontal* travel of length

$$\mathcal{L} = [1/\tan\theta + (1 - \mu/\tan\theta)(\cos^2\theta/\mu)]H \tag{3.2a}$$

$$\approx \mu^{-1} \qquad (\mu \ll \tan\theta; \cos\theta \approx 1). \tag{3.2b}$$

We first note from (3.2) that:

(i) $$\mathcal{L} \propto H; \tag{3.3a}$$

(ii) $$\mathcal{L}/H \text{ is independent of } M; \text{ and} \tag{3.3b}$$

(iii) $$\mathcal{L}/H \text{ is independent of } g. \tag{3.3c}$$

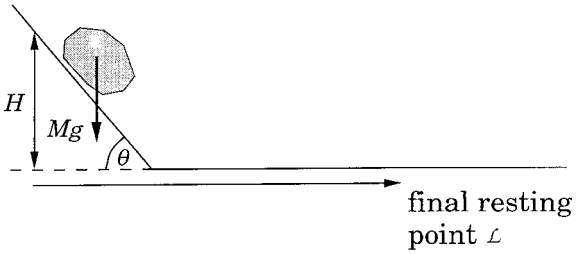

Figure 3. Sketch of a mass M, which slides down an inclined plane at an angle θ to the horizontal and then runs out at the base.

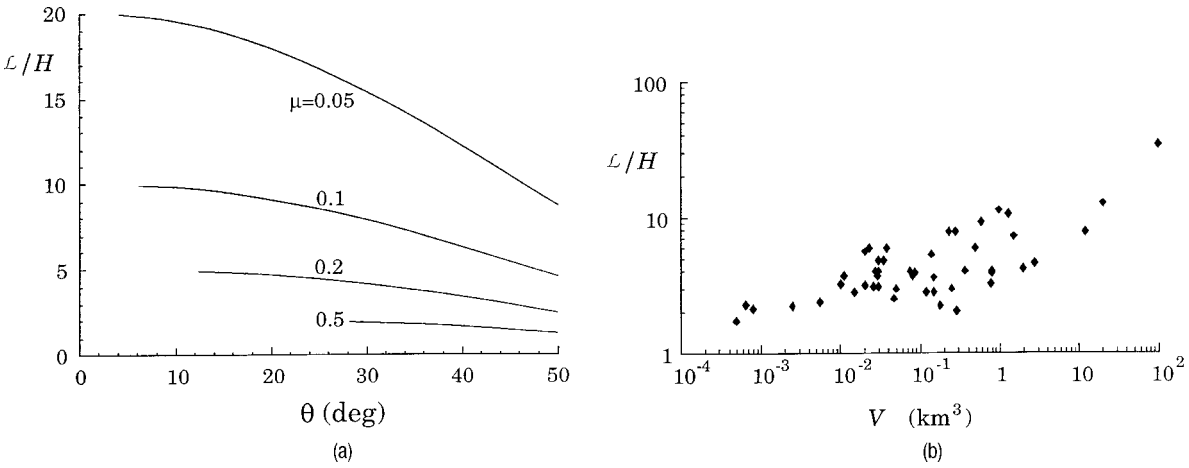

Figure 4. The ratio of the total horizontal runout distance $\mathcal{L}$ to the initial height above the base H: (a) as a function of the angle of the plane θ for a mass M, sliding down the plane; and (b) as a function of the volume V for observed rockslides.

Equation (3.4a) indicates that the runout is directly proportional to the fall height, while (3.4b and c) can also be obtained by dimensional arguments.

Figure 4(a) presents a plot of $\mathcal{L}/H$ as a function of θ for various values of μ. For a typical coefficient of sliding friction of 0.5 the horizontal runout is approximately 2. Equation (3.4b) suggests that $\mathcal{L}/H$ is independent of mass and hence volume of the fall, but it is instructive to plot the geological data for $\mathcal{L}/H$ as a function of the volume V (because θ does not vary over a wide range from one rockfall to another). The data from about 50 large rock avalanches and landslides are plotted in this way in Figure 4(b). It is immediately seen, as is well known, that $\mathcal{L}/H$ varies considerably, and systematically, with V. The above model is too simplistic to explain this variation. It does, however, indicate that long runouts correspond to effectively small coefficients of friction, and suggests that a low friction "fluid" model might be appropriate. Indeed, it is commonly stated that in the gigantic rockfalls, "the rocks flow as if like water".

Previous models of the scale dependence of $\mathcal{L}/H$ have been presented, including the suggestions that: trapped air could maintain the rocks in suspension (Shreve, 1968), but this would not work on the Moon or Mars; the rocks might melt to form a molten layer called "frictionite" (Erismann, 1979); or that high frequency vibrations could generate sufficient acoustical energy to diminish the effect of frictional contact between the rock surfaces (Melosh, 1979). None of these explanations has been generally accepted.

3.2. A Granular Flow Model

We summarize here the model, originally proposed by Dade *et al.* (1997), of the runout of a two-dimensional non-rigid array of rocks that travels uniformly above a thin region of intense particulate shear, on a horizontal boundary, as depicted in Figure 5. Rather than use the detailed descriptions of granular flow, as embodied in some of the work of Jenkins and Aavage (1983), Savage (1997), Anderson and Jackson (1992), and

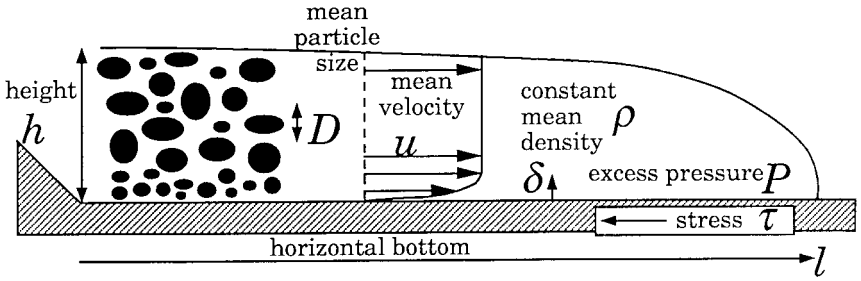

Figure 5. A sketch of the rock-laden current running along a horizontal base.

others, which make simplifying assumptions of their own and require the evaluation of a number of "free" parameters, we propose a direct model that is based on four main concepts. First, that the evolving rock flow satisfies a dynamic Coulomb condition at the base so that the ratio of normal forces to shear forces there is constant. Second, that the shear stress at the base is proportional to $\rho_r D^2(u/\delta)^2$, where ρ_r is the density of the rocks of *average* diameter D travelling at speed u in the interior flow above a boundary layer of thickness δ. This relationship was first proposed by Bagnold (1954), can be obtained by dimensional arguments and has been well confirmed in many experiments and "in just about every theoretical study" (Campbell, 1990). Third, that the particles in the boundary layer jostle about and hit each other in supporting the interior flow and thereby impart their horizontal momentum to the remaining flow as they drop out at the base with zero horizontal velocity. Finally, we assume that the Bagnold number $Ba = D(\tau/\rho)^{1/2}/\nu$ is large (greater than order 10^2), where τ is the shear stress at the base of the flow of mean density ρ and ν is the coefficient of kinematic viscosity of the interstitial fluid.

We envisage that the rock mass falls a height H down a slope θ and then spreads in two-dimensions across a horizontal floor in a disaggregated, non-rigid state. Over an 'entry' length l_0, defined in more detail below, the landslide organizes itself so as to be described by the following equations. These could be identified as averaged equations, somewhat akin to the box model equations of Section 2. In our view, it would be somewhat pointless to derive more complicated descriptions given that each rockfall is different in detail and that, in particular, the distribution of rock sizes varies considerably from one rockfall to another as does the terrain over which they flow.

In this spirit, we denote the total volume and mass at any time in the flow as $Q(t)$ and $M(t)$ where

$$Q = lh, \qquad M = \rho lh, \tag{3.4a,b}$$

and the flow is of length $l(t)$ and average thickness $h(t)$. The flow is resisted by a shear stress τ at the base, which we assume to be uniform. The equation of motion in terms of the mean velocity u then becomes

$$\frac{d}{dt}(Mu) = -\tau l, \tag{3.5}$$

which can be expanded to

$$\frac{du}{dt} = \frac{-\tau l}{M} - \frac{u}{M}\frac{dM}{dt}. \tag{3.6}$$

The first term on the right-hand side is negative and represents the deceleration of the flow due to frictional effects, while the second term is positive and represents the transfer of momentum to the flow from those rocks which because of collisions lose their horizontal velocity and then fall vertically to the base of the flow.

We evaluate τ by the Coulomb condition

$$\tau = kP = k\rho gh, \tag{3.7a,b}$$

where P is the pressure at the base of the flow due to the overlying weight and k is a constant generally taken to be about 0.5 (Campbell, 1990). As explained earlier

$$\tau = 2\rho_r D^2(u/\delta)^2, \tag{3.8}$$

where the pre-multiplicative constant follows the evaluation of Savage (1989).

Introducing a mean dynamic viscosity $\bar{\mu}$, defined by

$$\tau = \bar{\mu}u/\delta, \tag{3.9}$$

we can write (3.9) as

$$\bar{\mu} = 2\rho_r D^2(u/\delta) \tag{3.10}$$

and define a granular Reynolds number

$$Re = \rho u\delta/\bar{\mu} = \tfrac{1}{2}(\rho/\rho_r)(\delta/D)^2. \tag{3.11}$$

Laboratory experiments on the dimensions of a shear layer in a high-speed granular flow indicate that (δ/D)

lies between 5 and 15 (Hanes and Inman, 1985). In terms of this Reynolds number, τ can be written as

$$\tau = \beta\rho u^2, \qquad \beta = Re^{-1}. \tag{3.12a,b}$$

Thus the Reynolds number lies between approximately 5 and 50, while β takes on values between 0.02 and 0.2. The variation reflects the different distributions in rock properties, such as size and elastic rebound characteristics.

Substituting (3.12a) into (3.7) and using (3.4a), we obtain

$$Q = \beta l u^2/(kg), \tag{3.13}$$

which when substituted into (3.5), using (3.12) again, leads to

$$\frac{d}{dt}(lu^3) = -kglu^2. \tag{3.14}$$

Equation (3.14) needs to be solved subject to the initial condition

$$u = u_0 = (kgQ_0/\beta l_0)^{1/2} \qquad (l = l_0 = kgQ_0/\beta u_0^2), \tag{3.15}$$

where Q_0 is the initial volume of the flow, or, more accurately, the volume of the flow at the point l_0 beyond which the above governing equations are appropriate.

Converting the temporal derivative in (3.14) to a spatial derivative via $d/dt = ud/dl$ and introducing the non-dimensional velocity $W = u/u_0$ and distance $\xi = l/l_0$, we can express (3.14) and (3.15) as

$$(d/d\xi)(\xi W^3) = -\tfrac{5}{2}A\xi W, \tag{3.16}$$

$$W = 1 \qquad (\xi = 1), \tag{3.17}$$

where

$$A = \tfrac{2}{5}gkl_0/u_0^2 = \tfrac{2}{5}k(l_0/h_0)Fr_0^{-2} \tag{3.18}$$

in terms of the initial Froude number $Fr_0 = u_0/(gh_0)^{1/2}$ of the flow. With the substitution of a new variable $\psi = \xi W^3$ into (3.16), it can be readily solved along with (3.17) to yield

$$W = (1 + A - A\xi^{5/3})^{1/2}\xi^{-1/3}, \tag{3.19}$$

from which it follows from (3.13) that

$$Q/Q_0 = \xi W^2 = (1 + A - A\xi^{5/3})\xi^{1/3}. \tag{3.20}$$

The horizontal runout length L, at which $W = 0$ (and $Q = 0$), is given from (3.19) by

$$L = [(1 + A)A^{-1}]^{3/5}l_0 \equiv Bl_0, \tag{3.21}$$

where

$$l_0 = hgQ_0/\beta u_0^2 \sim \tfrac{1}{2}kQ_0/\beta H \tag{3.22a,b}$$

on the assumption that $u_0^2 \sim 2gH$. Inserting this expression and (3.22b) into (3.18), we find that

$$A \sim \tfrac{1}{10}k^2Q_0/\beta H^2. \tag{3.23}$$

Note, in passing, that both A and l_0 and hence L are independent of g (which is important only in determining the time *scale* of the flow), but that $\mathcal{L}/H$ is not independent of H (or of Q_0).

Inserting (3.22 b) into (3.21), we can finally write

$$\mathcal{L}/H = 1/\tan\theta + \tfrac{1}{2}kBQ_0/\beta H^2 \tag{3.24}$$

$$\sim 1/\tan\theta + \tfrac{1}{2}10^{3/5}(k\beta^2)^{-1/5}(Q_0/H^2)^{2/5} \qquad (Q_0 \ll H^2) \tag{3.25a}$$

$$\propto Q_0/H^2 \qquad (Q_0 \gg H^2), \tag{3.25b}$$

where (3.25a and b) correspond to relatively short and long runouts respectively.

Before comparing these results with field observations, we note that in the laboratory $H \sim 1$ m and so to achieve long runouts requires initial (two dimensional) volumes in considerable excess of 1 m^2. For an experimental chute of width 0.1m this corresponds to a three-dimensional volume of 0.1 m^3, which requires in excess of 100 kg of solid material, suggesting that laboratory simulation of such large rockfalls is nigh impossible.

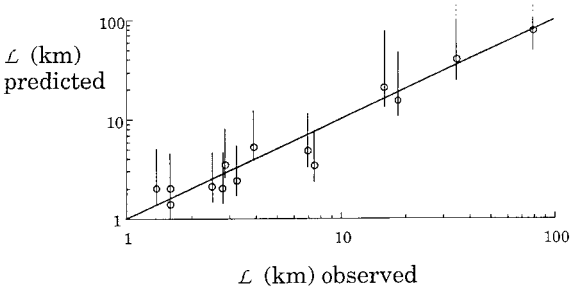

Figure 6. Predicted run out $\mathcal{L}$ as a function of the observed value for 14 rockfalls. The predicted lengths are calculated using a value of 0.1 for the inverse Reynolds number β with the error bars corresponding to a range of β from 0.02 to 0.2.

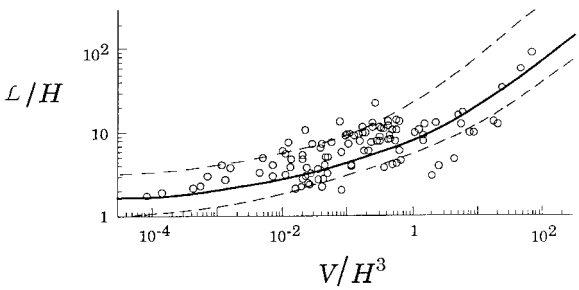

Figure 7. The ratio of runout length $\mathcal{L}$ to fall height H as a function of the ratio of initial volume V to H^3 for all the available rockfall data. The solid curve represents (3.26a) with $\beta = 0.1$ and $\theta = 35^0$. The dashed lines enclose the theoretical values for $20^0 < \theta < 50^0$ and $0.02 < \beta < 0.2$.

3.3. Comparisons with Field Data

The model we have developed is strictly two-dimensional. To compare the results with observations of real events we assume that, as first suggested by Campbell *et al*. (1995), such debris flows can be approximated as slowly-varying two-dimensional flows with average width proportional to the cube root of the initial three-dimensional volume V_0. This suggests that $Q_0^{1/2}$ should be replaced by $V_0^{1/3}$ in the above equations, leading to

$$\mathcal{L}/H = 1/\tan\theta + \tfrac{1}{2}kBV_0^{2/3}/\beta H^2 \tag{3.26a}$$

$$\sim 1/\tan\theta + \tfrac{1}{2}10^{3/5}(k\beta^2)^{-1/5}(V_0/H^3)^{4/15} \qquad (V_0 \ll H^3) \tag{3.26b}$$

$$\propto (V_0/H^3)^{2/3} \qquad (V_0 \gg H^3). \tag{3.26c}$$

Figure 6 plots predicted against observed lengths over two orders of magnitude for a number of rockfalls where the predicted lengths are calculated assuming $\beta = 0.1$ and error bars correspond to variations in β from 0.02 to 0.2. The straight line helps to confirm the agreement between the two axes. Some of the data, along with further details, are presented in Table 1. Figure 7 plots all the observations available to us of $\mathcal{L}/H$ as a function of V/H^3 along with the theoretical relationship (3.26a) evaluated for $\theta = 35°$ and $\beta = 0.1$. The dashed line encompasses values for which the model parameters span the ranges $20° < \theta < 50°$ and $0.02 < \beta < 0.2$. While there is some scatter in the data, as would be expected given the wide range in terrain, rock types, and sizes, the agreed trend between the model and the observations is in general encouraging.

4. Conclusions

We have reviewed two fluid-like models of distinctly solid flows. The first analysed the advection and sedimentation of small particles whose presence drove a gravity current. We explained how such flows can describe the extremely energetic pyroclastic flows which can result from large, violent volcanic eruptions. The second model analysed the energetic motion associated with large rockfalls. We showed that the model

Table 1. Observation (theory).

Name	V (km^3)	H (m)	θ (°)	$\mathcal{L}$ (km)	$\overline{u}$ (m s^{-1})	t (s)
Elm	0.01	610	45	1.6 (1.4)	(43)	(33)
Frank	0.03	870	45	1.6 (2.0)	(50)	(40)
Blackhawk	0.4	1220	15	7 (5)	(80)	(60)
Saidmarreh	20	1500	20	16 (20)	(110)	(180)
Valles Marineris	18,000	5000	30	100 (100)	(125)	(800)

led to results for the runout length which are in good agreement with observational data. The last word has not been written in either situation. Building on our simple models, which we hope capture the most important aspects of the physics, we plan to incorporate further details of these fascinating, highly destructive flows in the future.

Acknowledgements

Many of our colleagues have helped us come to our current understanding of largescale geological disasters. We would like to thank particularly R.T. Bonnecaze, M.A. Hallworth, A.J. Hogg, J.R. Lister and R.S.J. Sparks, with whom we have co-authored papers on the subject, and also many others with whom we have had stimulating conversations.

We are grateful to P. Hall, C. Hunter and M.Y. Hussaini, the organisers of the International Symposium on Theoretical and Computational Fluid Dynamics in honour of James Lighthill, for inviting one of us (HEH) to attend the Symposium and allowing us to present our current work in this way.

Finally, it is a great pleasure to acknowledge James Lighthill's stimulating role model and his explicit help at a number of crucial points in the development of the career of one of us (HEH).

References

Anderson, K.G., and Jackson, R. (1992). A comparison of the solutions of some proposed equations of motion of granular materials for fully developed flow down inclined planes. *J. Fluid Mech.* **241**, 145–168.

Bagnold, R.A. (1954). Experiments on a gravity-free dispersion of large solid particles in a Newtonian fluid under shear. *Proc. Roy. Soc. London Ser. A* **225**, 49–63.

Benjamin, T.B. (1968). Gravity currents and related phenomena. *J. Fluid Mech.* **31**, 209–248.

Bonnecaze, R.T., Hallworth, M.A., Huppert, H.E., and Lister, J.R. (1995) Axisymmetric particle-driven gravity currents. *J. Fluid Mech.* **294**, 93–121.

Bonnecaze, R.T., Huppert, H.E., and Lister, J.R. (1996) Patterns of sedimentation from polydispersed turbidity currents. *Proc. Roy. Soc. London Ser. A* **452**, 2247–2261.

Campbell, C.S. (1990) Rapid granular flows. *Ann. Rev. Fluid Mech.* **22**, 57–92.

Campbell, C.S., Cleary, P.W., and Hopkins, M. (1995) Large-scale landslide simulations: global deformation, velocities and basal friction. *J. Geophys. Res.* **100**, 8267–8273.

Dade, W.B., and Huppert, H.E. (1995) Runout and fine-sediment deposits of axisymmetric gravity currents. *J. Geophys. Res. (Oceans)* **100**, 18,597–18,609.

Dade, W.B., and Huppert, H.E. (1996) Emplacement of the Taupo ignimbrite by a dilute turbulent flow. *Nature* **381**, 509–512.

Dade, W.B., and Huppert, H.E. (1997) Emplacement of the Taupo ignimbrite—reply. *Nature* **385**, 306–307.

Dade, W.B., Hogg, A.J., and Huppert, H.E. (1997) Long-runout rockfalls *J. Geophys. Res.* (submitted).

Dobran, F., Neri, A., and Macedonio, G. (1993) Numerical simulation of collapsing volcanic columns. *J. Geophys. Res.* **98**, 4231–4259.

Dobran, F., Neri, A., and Todesco, M. (1994) Assessing the pyroclastic flow hazard at Vesuvius. *Nature* **367**, 551–554.

Erismann, T.H. (1979) Mechanisms of large landslides. *Rock Mech.* **12**, 5–46.

Francis, P. (1993) *Volcanoes.* Oxford University Press, Oxford.

Hanes, D.M., and Inman, D.L. (1985) Observations of rapidly flowing granular-fluid mixtures. *J. Fluid Mech.* **150**, 357–380.

Kármán, T.von (1940) The engineer grapples with non-linear problems. *Bull. Am. Math. Soc.* **46**, 615–683.

Kieffer, S. (1977) Sound speed in liquid-gas mixtures: water-air and water-steam. *J. Geophys. Res.* **82**, 2895–2904.

Lighthill, M.J., Zhemin, Z., Holland, G., and Emanuel, K. (1993) *Tropical Cyclone Disasters.* Peking University Press, Beijing.

Lighthill, M.J. (1996) *Typhoons, Hurricanes and Fluid Mechanics.* Proc XIX ICTAM Kyoto, 1996, Kluever, Dordrecht.

Lucchitta, B.K. (1979) Landslides in Valles Marineris, Mars. *J. Geophys. Res.* **84**, 8097–8113.

Martin, D., and Nokes, R. (1988) Crystal settling in a vigorously convecting magma chamber. *Nature* **332**, 534–536.

Melosh, H.J. (1979) Acoustic fluidization: a new geological process? *J. Geophys. Res.* **84**, 7513–7520.

Pliny, the Younger (79) *The Letters of the Younger Pliny Translated by B. Radice.* Penguin Classics.

Rampino, M.R. (1992) Volcanic hazards. In: *Understanding the Earth*, Brown, G.C., Hawkesworth, C.J., and Wilson, R.C.L. (eds.). Cambridge University Press, Cambridge, pp. 506–522.

Savage, S.B. (1989) *Flow of Granular Materials.* IUTAM Theoretical and Applied Mechanics. Elsevier, Amsterdam, pp. 241–266.

Savage, S.B. (1997) Analyses for slow, quasi-static, high concentration flows of granular materials. *J. Fluid Mech.* (submitted).

Shreve, R.L. (1968) *The Blackhawk Landslide*. Special Papers of the Geological Society of America, Vol. 108, 47 pp.

Simpson, J.E. (1997) *Gravity currents in the Environment and the Laboratory.* Cambridge University Press, 244 pp.

Wilson, C.J.N. (1985) The Taupo eruption, New Zealand II. The Taupo ignimbrite *Philos. Trans. Roy. Soc. London Ser. A* **314**, 229–310.

Wilson, C.J.N. (1997) Emplacement of Taupo ignimbrite. *Nature* **385**, 306.

Wilson, C.J.N., Houghton, B.F., Kamp, P.J.J., and McWilliams, M.O. (1995) An exceptionally widespread ignimbrite with implication for pyroclastic flow emplacement. *Nature* **378**, 605–607.

Woods, A.W. (1988) The fluid dynamics and thermodynamics of eruption columns. *Bull. Volcanol.* **50**, 169–193.

Woods, A.W. (1995) The dynamics of explosive volcanic eruptions. *Rev. Geophys.* **33**, 495–530.